

Dual Shell-like Magnetic Clusters Containing Ni^{II} and Ln^{III} (Ln = La, Pr, and Nd) IonsXiang-Jian Kong,[†] Yan-Ping Ren,[†] La-Sheng Long,^{*,†} Zhiping Zheng,^{*,†} Gary Nichol,[‡] Rong-Bin Huang,[†] and Lan-Sun Zheng[†]

State Key Laboratory of Physical Chemistry of Solid Surface and Department of Chemistry, College of Chemistry and Chemical Engineering, Xiamen University, Xiamen 361005, China, and Department of Chemistry, University of Arizona, Tucson, Arizona 85721

Received October 19, 2007

Dual shell-like nanoscopic magnetic clusters featuring a polynuclear nickel(II) framework encapsulating that of lanthanide ions (Ln = La, Pr, and Nd) were synthesized using Ni(NO₃)₂ · 6H₂O, Ln(NO₃)₃ · 6H₂O, and iminodiacetic acid (IDA) under hydrothermal conditions. Structurally established by crystallographic studies, these clusters are [La₂₀Ni₃₀(IDA)₃₀(CO₃)₆(NO₃)₆(OH)₃₀(H₂O)₁₂](CO₃)₆ · 72H₂O (**1**), [Ln₂₀Ni₂₁(C₂H₅NO₄)₂₁(OH)₂₄(C₂H₂O₃)₆(C₂O₄)₃(NO₃)₉ · (H₂O)₁₂](NO₃)₉ · nH₂O [C₂H₂O₃ is the alkoxide form of glycolate; Ln = Pr (**2**), n = 42; Nd (**3**), n = 50], and {[La₄Ni₅Na(IDA)₅(CO₃)(NO₃)₄(OH)₅(H₂O)₅][CO₃] · 10H₂O}_∞ (**4**). Carbonate, oxalate, and glycolate are products of hydrothermal decomposition of IDA. Compositions of these compounds were confirmed by satisfactory elemental analyses. It has been found that the cluster structure is dependent on the identity of the lanthanide ion as well as the starting Ln/Ni/IDA ratio. The cationic cluster of **1** features a core of the Keplerate type with an outer icosidodecahedron of Ni^{II} ions encaging a dodecahedral kernel of La^{III}. Clusters **2** and **3**, distinctly different from **1**, are isostructural, possessing a core of an outer shell of 21 Ni^{II} ions encapsulating an inner shell of 20 Ln^{III} ions. Complex **4** is a three-dimensional assembly of cluster building blocks connected by units of Na(NO₃)/La(NO₃)₃; the structure of the building block resembles closely that of **1**, with a hydrated La^{III} ion internalized in the decanuclear cage being an extra feature. Magnetic studies indicated ferromagnetic interactions in **1**, while overall antiferromagnetic interactions were revealed for **2** and **3**. The polymeric, three-dimensional cluster network **4** displayed interesting ferrimagnetic interactions.

Introduction

High-nuclearity metal complexes are enjoying widespread current interest not only because of their nanoscale and aesthetically pleasing molecular structures but also because of their interesting properties and envisioned technological applications.¹ The design, synthesis, and structural characterization of such substances present a fundamental challenge for synthetic and structural chemists. Efforts in the past 2 decades or so have resulted in a large number of such complexes whose structural beauty is reflected by such unique architectures as wheels,² ladders,³ tubes,⁴ and helices.⁵ The unique arrangement of the multiple metal centers within the complex framework, together with the inherently inter-

esting traits of the individual metal ions, often leads to attractive properties not available in their mononuclear or lower-nuclearity analogues. Arguably most notable are the novel magnetic phenomena exhibited by many of these

* To whom correspondence should be addressed. E-mail: lslong@xmu.edu.cn (L.-S.L.), zhiping@u.arizona.edu (Z.Z.).

[†] Xiamen University.

[‡] University of Arizona.

- (1) (a) Andruh, M. *Chem. Commun.* **2007**, 25, 2565. (b) Ruiz, R.; Faus, J.; Lloret, F.; Julve, M.; Journaux, Y. *Coord. Chem. Rev.* **1999**, 193(195), 1069. (c) Stamatatos, T. C.; Christou, A. G.; Jones, C. M.; O'Callaghan, B. J.; Abboud, K. A.; O'Brien, T. A.; Christou, G. *J. Am. Chem. Soc.* **2007**, 129, 9840. (d) McInnes, E. J. L.; Piligkos, S.; Timco, G. A.; Winpenny, R. E. P. *Coord. Chem. Rev.* **2005**, 249, 2577. (e) Cooke, M. W.; Hanan, G. S. *Chem. Soc. Rev.* **2007**, 36, 1466. (f) Kornienko, A.; Emge, T. J.; Kumar, G. A.; Riman, R. E.; Brennan, J. G. *J. Am. Chem. Soc.* **2005**, 127, 3501. (g) Beltran, L. M. C.; Long, J. R. *Acc. Chem. Res.* **2005**, 38, 325. (h) Verdagner, M. *Science* **1996**, 272, 698. (i) Mrozinski, J. *Coord. Chem. Rev.* **2005**, 249, 2534. (j) Schelter, E. J.; Prosvirin, A. V.; Dunbar, K. R. *J. Am. Chem. Soc.* **2004**, 126, 15004. (k) Caneschi, A.; Gatteschi, D.; Lalioti, N.; Sangregorio, C.; Sessoli, R.; Venturi, G.; Vindigni, A.; Rettori, A.; Pini, M. G.; Novak, M. *Angew. Chem., Int. Ed.* **2001**, 40, 1760. (l) Clérac, R.; Miyasaka, H.; Yamashita, M.; Coulon, C. *J. Am. Chem. Soc.* **2002**, 124, 12837.

complexes, among which single-molecule magnets⁶ and single-chain magnets⁷ have received much recent interest. The ability to construct even higher-order extended systems using such individual clusters as building blocks offers even more opportunities for structural studies and property investigation.

Polynuclear heterometallic complexes featuring both transition metals and f elements occupy a special position in this context because it is possible to generate systems with high ground-state spin states and magnetic anisotropy as a result of the unique electronic configurations of these metals.⁸ Indeed, much of the recent work on the synthesis and magnetostructural studies of high-nuclearity complexes has been devoted to the assembly of such heterometallic systems. Structurally interesting discrete cluster-type complexes as well as assemblies using well-defined complexes or clusters of transition metals and f elements as building blocks have

been realized.⁹ Magnetic studies of such complexes have resulted in a better understanding of the exchange interactions between different metal ions and the contribution of the f elements to the overall magnetic properties of the heterometallic systems, with the discovery of lanthanide-containing single-molecule magnets being a recent highlight of such efforts.¹⁰ We note that the preponderance of the work is with the use of the lanthanide ions, but complexes featuring actinide elements have also appeared recently in the literature.¹¹

Two general routes have been utilized to synthesize polynuclear complexes of mixed metals. In the first approach, a preformed complex of a transition metal is used as a ligand for the coordination of the lanthanide ion.¹² Such an approach is particularly useful for the synthesis of bimetallic complexes. Generally, a specially designed ligand featuring distinct coordinating compartments, respectively for preferential binding of transition metals and the lanthanides, is needed. In a second approach, one-pot synthesis using a mixture of the starting metal salts and certain judiciously chosen ligands leads to the assembly of heterometallic complexes. This latter approach has enjoyed great success recently, with which many high-nuclearity complexes have

- (2) (a) Cador, O.; Gatteschi, D.; Sessoli, R.; Larsen, F. K.; Overgaard, J.; Barra, A.-L.; Teat, S. J.; Timco, G. A.; Winpenny, R. E. P. *Angew. Chem., Int. Ed.* **2004**, *43*, 5196. (b) Manoli, M.; Prescimone, A.; Bagai, R.; Mishra, A.; Murugesu, M.; Parsons, S.; Wernsdorfer, W.; Christou, G.; Brechin, E. K. *Inorg. Chem.* **2007**, *46*, 6968. (c) Müller, A.; Pope, M. T.; Todea, A. M.; Bögge, H.; van Slageren, J.; Dressel, M.; Gouzerh, P.; Thouvenot, R.; Tsukerblat, B.; Bell, A. *Angew. Chem., Int. Ed.* **2007**, *46*, 4477. (d) Saalfrank, R. W.; Scheurer, A.; Prakash, R.; Heinemann, F. W.; Nakajima, T.; Hampel, F.; Leppin, R.; Pilawa, B.; Rupp, H.; Müller, P. *Inorg. Chem.* **2007**, *46*, 1586. (e) Chen, X.-Y.; Bretonniere, Y.; Pecaut, J.; Imbert, D.; Buenzli, J.-C.; Mazzanti, M. *Inorg. Chem.* **2007**, *46*, 625. (f) Cheng, J.-W.; Zhang, J.; Zheng, S.-T.; Zhang, M.-B.; Yang, G.-Y. *Angew. Chem., Int. Ed.* **2006**, *45*, 73. (g) Gamer, M. T.; Roesky, P. W. *Inorg. Chem.* **2005**, *44*, 5963. Müller, A.; Krickemeyer, E.; Meyer, J.; Bögge, H.; Peters, F.; Plass, W.; Diemann, E.; Dillinger, S.; Nonnenbruch, F.; Randerath, M.; Menke, C. *Angew. Chem., Int. Ed.* **1995**, *34*, 2122. (i) Taft, K. L.; Delfs, C. D.; Papaefthymiou, G. C.; Foner, S.; Gatteschi, D.; Lippard, S. J. *J. Am. Chem. Soc.* **1994**, *116*, 823. (j) Dolbecq, A.; Secheresse, F. *Adv. Inorg. Chem.* **2002**, *53*, 1. (k) Wang, R.; Selby, H. D.; Liu, H.; Carducci, M. D.; Jin, T.; Zheng, Z.; Anthis, J. W.; Staples, R. J. *Inorg. Chem.* **2002**, *41*, 278. (l) Botar, B.; Koegerler, P.; Hill, C. L. *J. Am. Chem. Soc.* **2006**, *128*, 5336.
- (3) (a) Wang, Y.; Ding, B.; Cheng, P.; Liao, D.-Z.; Yan, S.-P. *Inorg. Chem.* **2007**, *46*, 2002. (b) Antonioli, B.; Clegg, J. K.; Bray, D. J.; Gloe, K.; Gloe, K.; Hesske, H.; Lindoy, L. F. *CrystEngComm.* **2006**, *8*, 748. (c) Lu, X.-Q.; Jiang, J.-J.; zur Loye, H.-C.; Kang, B.-S.; Su, C.-Y. *Inorg. Chem.* **2005**, *44*, 1810. (d) Zou, Y.; Liu, W.; Gao, S.; Xie, J.; Meng, Q. *Chem. Commun.* **2003**, *23*, 2946. (e) Losier, P.; Zaworotko, M. J. *Angew. Chem., Int. Ed.* **1997**, *35*, 2779. (f) Gamez, P.; de Hoog, P.; Roubeau, O.; Lutz, M.; Driessen, W. L.; Spek, A. L.; Reedijk, J. *Chem. Commun.* **2002**, *14*, 1488.
- (4) (a) Schmittel, M.; Kalsani, V.; Michel, C.; Mal, P.; Ammon, H.; Jaeckel, F.; Rabe, J. P. *Chem.—Eur. J.* **2007**, *13*, 6223. (b) Fujita, M.; Tominaga, M.; Hori, A.; Therrien, B. *Acc. Chem. Res.* **2005**, *38*, 369. (c) Atwood, J. L.; Barbour, L. J.; Hardie, M. J.; Raston, C. L. *Coord. Chem. Rev.* **2001**, *222*, 3.
- (5) (a) Wu, S.-T.; Wu, Y.-R.; Kang, Q.-Q.; Zhang, H.; Long, L.-S.; Zheng, Z.; Hunag, R. B.; Zheng, L.-S. *Angew. Chem., Int. Ed.* **2007**, *46*, in press (DOI: 10.1002/anie.200703443). (b) Feng, Y.; Guo, Y.; OuYang, Y.; Liu, Z.; Liao, D.; Cheng, P.; Yan, S.; Jiang, Z. *Chem. Commun.* **2007**, *35*, 3643. (c) Horikoshi, R.; Mochida, T. *Coord. Chem. Rev.* **2006**, *250*, 2595. (d) Miyake, H.; Tsukube, H. *Supramol. Chem.* **2005**, *17*, 53. (e) Ziessel, R. *Coord. Chem. Rev.* **2001**, *216*(217), 195. (f) Williams, A. *Chem.—Eur. J.* **1997**, *3*, 15.
- (6) (a) Christou, G. *Polyhedron* **2005**, *24*, 2065. (b) Cornia, A.; Costantino, A. F.; Zoppi, L.; Caneschi, A.; Gatteschi, D.; Mannini, M.; Sessoli, R. *Struct. Bonding (Berlin)* **2006**, *122*, 133. (c) Lescouezec, R.; Toma, L. M.; Vaissermann, J.; Verdager, M.; Delgado, F. S.; Ruiz-Perez, C.; Lloret, F.; Julve, M. *Coord. Chem. Rev.* **2005**, *249*, 2691.
- (7) (a) Coulon, C.; Miyasaka, H.; Clerac, R. *Struct. Bonding (Berlin)* **2006**, *122*, 163. (b) Miyasaka, H.; Clerac, R. *J. Chem. Soc. Jpn.* **2005**, *78*, 1725. (c) Bernot, K.; Bogani, L.; Sessoli, R.; Gatteschi, D. *Inorg. Chim. Acta* **2007**, *360*, 3807. (d) Liu, T.; Fu, D.; Gao, S.; Zhang, Y.; Sun, H.; Su, G.; Liu, Y. *J. Am. Chem. Soc.* **2003**, *125*, 13976.
- (8) Benelli, C.; Gatteschi, D. *Chem. Rev.* **2002**, *102*, 2369.
- (9) (a) Winpenny, R. E. P. *Chem. Soc. Rev.* **1998**, *27*, 447. (b) Xu, Z.; Read, P. W.; Hibbs, D. E.; Hursthouse, M. B.; Abdul Malik, K. M.; Patrick, B. O.; Rettig, S. J.; Seid, M.; Summers, D. A.; Pink, M.; Thompson, R. C.; Orvig, C. *Inorg. Chem.* **2000**, *39*, 508. (c) Wu, G.; Hewitt, I. J.; Mameri, S.; Lan, Y.; Clérac, R.; Anson, C. E.; Qiu, S.; Powell, A. K. *Inorg. Chem.* **2007**, *46*, 7229. (d) Osa, S.; Kido, T.; Matsumoto, N.; Re, N.; Pochaba, A.; Mrozinski, J. *J. Am. Chem. Soc.* **2004**, *126*, 420. (e) Gheorghie, R.; Cucos, P.; Andruh, M.; Costes, J.-P.; Donnadieu, B.; Shova, S. *Chem.—Eur. J.* **2005**, *12*, 187. (f) Zhao, B.; Cheng, P.; Chen, X.; Cheng, C.; Shi, W.; Liao, D.; Yan, S.; Jiang, Z. *J. Am. Chem. Soc.* **2004**, *126*, 3012. (g) Akine, S.; Taniguchi, T.; Nabeshima, T. *Angew. Chem., Int. Ed.* **2002**, *41*, 4670.
- (10) (a) Zaleski, C. M.; Depperman, E. C.; Kampf, J. W.; Kirk, M. L.; Pecoraro, V. L. *Angew. Chem., Int. Ed.* **2004**, *43*, 3912. (b) Ferbinteanu, M.; Kajiwaru, T.; Choi, K.; Nojiri, H.; Nakamoto, A.; Kojima, N.; Cimpoesu, F.; Fujimura, Y.; Takaiishi, S.; Yamashita, M. *J. Am. Chem. Soc.* **2006**, *128*, 9008. (c) Mori, F.; Nyui, T.; Ishida, T.; Nogami, T.; Choi, K.; Nojiri, H. *J. Am. Chem. Soc.* **2006**, *128*, 1440. (d) Mishra, A.; Wernsdorfer, W.; Parsons, S.; Christou, G.; Brechin, E. K. *Chem. Commun.* **2005**, *16*, 2086. (e) Mishra, A.; Wernsdorfer, W.; Abboud, K. A.; Christou, G. *J. Am. Chem. Soc.* **2004**, *126*, 15648. (f) Tasiopoulos, A. J.; O'Brien, T.; Abboud, K. A.; Christou, G. *Angew. Chem., Int. Ed.* **2004**, *43*, 345. (g) Mereacre, V. M.; Aho, A. M.; Clerac, R.; Wernsdorfer, W.; Filoti, G.; Bartolome, J.; Anson, C. E.; Powell, A. K. *J. Am. Chem. Soc.* **2007**, *129*, 9248. (h) Ishikawa, N. *Polyhedron* **2007**, *26*, 2147. (i) Costes, J.-P.; Auchel, M.; Dahan, F.; Peyrou, V.; Shova, S.; Wernsdorfer, W. *Inorg. Chem.* **2006**, *45*, 1924. (j) Ishikawa, N.; Sugita, M.; Wernsdorfer, W. *J. Am. Chem. Soc.* **2005**, *127*, 3650.
- (11) (a) Kozimor, S. A.; Bartlett, B. M.; Rinehart, J. D.; Long, J. R. *J. Am. Chem. Soc.* **2007**, *129*, 10672. (b) Mishra, A.; Tasiopoulos, A. J.; Wernsdorfer, W.; Abboud, K. A.; Christou, G. *Inorg. Chem.* **2007**, *46*, 3105. (c) Mishra, A.; Abboud, K. A.; Christou, G. *Inorg. Chem.* **2006**, *45*, 2364. (d) Schelter, E. J.; Veauthier, J. M.; Thompson, J. D.; Scott, B. L.; John, K. D.; Morris, D. E.; Kiplinger, J. L. *J. Am. Chem. Soc.* **2006**, *128*, 2198. (g) Salmon, L.; Thury, P.; Riviere, E.; Ephritikhine, M. *Inorg. Chem.* **2006**, *45*, 83.
- (12) (a) Caneschi, A.; Sorace, L.; Casellato, U.; Tomasin, P.; Vigato, P. A. *Eur. J. Inorg. Chem.* **2004**, *19*, 3887. (b) Shavaleev, N. M.; Pope, S. J. A.; Bell, Z. R.; Faulkner, S.; Ward, M. D. *Dalton Trans.* **2003**, *5*, 808. (c) Botta, M.; Casellato, U.; Scalco, C.; Tamburini, S.; Tomasin, P.; Vigato, P. A.; Aime, S.; Barge, A. *Chem.—Eur. J.* **2002**, *8*, 3917. (d) Koner, R.; Lin, H.-H.; Wei, H.-H.; Mohanta, S. *Inorg. Chem.* **2005**, *44*, 3524. (e) Kahn, M. L.; Mathonière, C.; Kahn, O. *Inorg. Chem.* **1999**, *38*, 3692. (f) Costes, J.-P.; Dupuis, A.; Laurent, J.-P. *Chem.—Eur. J.* **1998**, *1616*. (g) Figuerola, A.; Diaz, C.; Ribas, J.; Tangoulis, V.; Granell, J.; Lloret, F.; Mahia, J.; Maestro, M. *Inorg. Chem.* **2003**, *42*, 641.

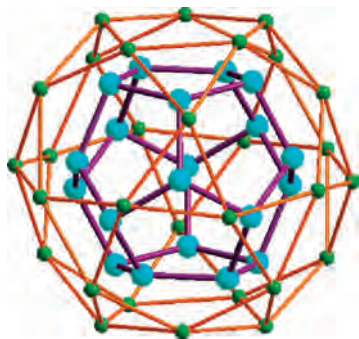


Figure 1. Cluster core structure of **1** showing an outer Ni₃₀ icosidodecahedron encapsulating an inner La₂₀ dodecahedron. Color legends: Ni, green; La, cyan.

been obtained.¹³ Frequently present in these nanoscale cluster-type polynuclear complexes are water-derived ligands, in particular hydroxo groups, presumably due to the hydrolysis of the metal ions limited by the organic supporting ligands.¹⁴

We have been interested in the synthesis of polynuclear metal complexes and their magnetic property studies. Utilizing a mixture of La(NO₃)₃, Ni(NO₃)₂, and iminodiacetic acid, hydrothermal synthesis yielded a gigantic mixed-metal cluster [La₂₀Ni₃₀(IDA)₃₀(CO₃)₆(NO₃)₆(OH)₃₀(H₂O)₁₂](CO₃)₆ (**1**) (IDA = iminodiacetate). Crystallographic analysis revealed the fascinating double-sphere structure of the cluster core with the outer sphere of 30 Ni^{III} ions encapsulating the inner sphere of 20 La^{III} ions (Figure 1).¹⁵ The 30 Ni^{III} ions span an icosidodecahedron, one of the Archimedean solids formed by 12 pentagonal and 20 triangular faces, while the 20 La^{III} ions occupy the vertices of a perfect dodecahedron, one of the Platonic solids featuring 12 pentagonal faces. The term of “Keplerate” has been used by Müller and co-workers to describe such a structure that features Platonic and Archimedean solids one inside another.¹⁶ The cagelike arrangement of the two distinct sets of metal ions manifests the beauty of symmetry because both ideally possess icosahedral (*I_h*) symmetry, the highest possible symmetry for molecules.¹⁷

The structural aesthetics is comparable to that of the celebrated nanocapsule of polyoxometalates,¹⁶ the fullerene-like clusters,^{18,19} and the Pd₁₄₅ cluster.²⁰

Cluster **1** constitutes a framework of Ni^{II} centers with an unusual spin topology as in the case of the seminal Mo₇₂Fe₃₀ cluster¹⁷ and its analogues.²¹ Temperature-dependent susceptibility measurements indicated an overall ferromagnetic interaction between the Ni^{II} ions.¹⁵

The structural beauty and intriguing magnetic behavior of this gigantic cluster stimulated our further interest in this class of complexes. The seemingly readily extendable synthetic methodology coupled with the rich variety of transition metals and the lanthanide elements suggest abundant opportunities for the preparation and property investigation of nanoscopic magnetic clusters of similar types. Synthetically, structural analogues of **1** by featuring other lanthanide and/or transition-metal ions can be anticipated. Clusters of different structural types may be possible because of the difference in size and Lewis acidity of the metal ions, especially for the lanthanide ions. In terms of materials properties, the diverse electronic configurations of these metal ions suggest a great potential for systematic and comparative property investigation of these clusters. It is also tempting to consider the assembly of a higher-order supramolecular structure by using the discrete cluster as building blocks,²² analogous to the assembly of Mo₇₂Fe₃₀ by Müller,¹⁶ that of Mn₈₄ cluster by Christou et al.,²³ and that of Co₄O₄ cubes by Chen et al.²⁴ This will enable the creation and manipulation of cooperative interactions among individual high ground-state spin complexes in a controlled fashion.^{1a,25}

Results based on our efforts along these lines of thinking are reported in this work. Specifically, we describe the synthesis, structural characterization by single-crystal X-ray diffraction, and magnetic studies of three new cluster complexes, of which two are isostructural but distinctly different from **1**, consisting of 21 Ni^{II} ions and 20 Pr^{III} (**2**) or 20 Nd^{III} (**3**) ions. The third compound (**4**) is a three-dimensional cluster assembly of cluster building blocks connected by units of Na(NO₃)/La(NO₃)₃; the structure of the building block resembles closely that of **1**, with an additional hydrated La^{III} ion internalized in the decanuclear La^{III} cage. The structure and magnetic studies of cluster **1**,

- (13) (a) Bagai, R.; Abboud, K. A.; Christou, G. *Inorg. Chem.* **2007**, *46*, 5567. (b) Smith, A. A.; Coxall, R. A.; Harrison, A.; Helliwell, M.; Parsons, S.; Winpenny, R. E. P. *Polyhedron* **2004**, *23*, 1557. (c) Milius, C. J.; Kefalloniti, E.; Raptopoulou, C. P.; Terzis, A.; Vicente, R.; Lalioti, N.; Escuer, A.; Perlepes, S. P. *Chem. Commun.* **2003**, 819. (d) Boyle, T. J.; Tyner, R. P.; Alam, T. M.; Scott, B. L.; Ziller, J. W.; Potter, B. G., Jr. *J. Am. Chem. Soc.* **1999**, *121*, 12104. (e) Beer, R. H.; Lippard, S. J. *Inorg. Chem.* **1993**, *32*, 1030. (f) Schmitt, H.; Lomoth, R.; Magnuson, A.; Park, J.; Fryxell, J.; Kritikos, M.; Martensson, J.; Hammarstrom, L.; Sun, L.; Akermark, B. *Chem.—Eur. J.* **2002**, *8*, 3757.
- (14) (a) Zheng, Z. *Chem. Commun.* **2001**, 2521. (b) Zheng, Z. *Chemtracts* **2003**, *16*, 1.
- (15) Kong, X.-J.; Ren, Y.-P.; Long, L.-S.; Zheng, Z.; Huang, R.-B.; Zheng, L.-S. *J. Am. Chem. Soc.* **2007**, *129*, 7016.
- (16) (a) Müller, A. *Nature* **2007**, *447*, 1035. (b) Müller, A.; Krickemeyer, E.; Bogge, H.; Schmidtman, M.; Peters, F. *Angew. Chem., Int. Ed.* **1998**, *37*, 3360. (c) Müller, A.; Kögerler, P.; Dress, A. *Coord. Chem. Rev.* **2001**, *222*, 193. (d) Müller, A.; Sarkar, S.; Shah, S. Q. N.; Bögge, H.; Schmidtman, M.; Sarkar, S.; Kögerler, P.; Hauptfleisch, B.; Trautwein, A. X.; Schünemann, V. *Angew. Chem., Int. Ed.* **1999**, *38*, 3238. (e) Müller, A.; Luban, M.; Schröder, C.; Modler, R.; Kögerler, P.; Axenovich, M.; Schnack, J.; Canfield, P.; Bud'ko, S.; Harrison, N. *ChemPhysChem* **2001**, *2*, 517. (f) Müller, A.; Shah, S. Q. N.; Bogge, H.; Schmidtman, M. *Nature* **1999**, *397*, 48.
- (17) O’Keeffe, M.; Hyde, B. G. *Crystal Structures, I: Patterns and Symmetry*; Mineralogical Society of America: Washington, DC, 1996.

- (18) Bai, J.; Virovets, A. V.; Scheer, M. *Science* **2003**, *300*, 781.
- (19) Moses, M. J.; Fettingler, J. C.; Eichhorn, B. W. *Science* **2003**, *300*, 778.
- (20) (a) Mednikov, E. G.; Jewell, M. C.; Dahl, L. F. *J. Am. Chem. Soc.* **2007**, *129*, 11619. (b) Tran, N. T.; Powell, D. R.; Dahl, L. F. *Angew. Chem., Int. Ed.* **2000**, *39*, 4121.
- (21) (a) Botar, B.; Kögerler, P.; Hill, C. L. *Chem. Commun.* **2005**, 3138. (b) Müller, A.; Todea, A. M.; Dressel, M.; van Slageren, J.; Bögge, H.; Schmidtman, M.; Luban, M.; Engelhardt, L.; Rusu, M. *Angew. Chem., Int. Ed.* **2005**, *44*, 3857.
- (22) (a) Huang, D.; Zhang, X.; Ma, C.; Chen, H.; Chen, C.; Liu, Q.; Zhang, C.; Liao, D.; Li, L. *Dalton Trans.* **2007**, 680. (b) Wernsdorfer, W.; Aliaga-Alcalde, N.; Hendrickson, D. N.; Christou, G. *Nature* **2002**, *416*, 406. (c) Müller, A.; Das, S. K.; Kögerler, P.; Bögge, H.; Schmidtman, M.; Trautwein, A. X.; Schünemann, V.; Krickemeyer, E.; Preetz, W. *Angew. Chem., Int. Ed.* **2000**, *39*, 3413.
- (23) Tasiopoulos, A. J.; Vinslava, A.; Wernsdorfer, W.; Abboud, K. A.; Christou, G. *Angew. Chem., Int. Ed.* **2004**, *43*, 2117.
- (24) Zeng, M.; Yao, M.; Liang, H.; Zhang, W.; Chen, X. *Angew. Chem., Int. Ed.* **2007**, *46*, 1832.
- (25) Miyasaka, H.; Yamashita, M. *Dalton Trans.* **2007**, 399.

Table 1. Crystallographic Data and Details of Data Collection and Refinement for 1–4

	1	2	3	4
formula	C ₁₃₂ H ₃₄₈ La ₂₀ N ₃₆ Ni ₃₀ O ₂₈₈	C ₁₀₂ H ₂₄₉ N ₃₉ Ni ₂₁ O ₂₄₆ Pr ₂₀	C ₁₀₂ H ₂₆₅ N ₃₉ Nd ₂₀ Ni ₂₁ O ₂₅₄	C ₁₃₂ H ₃₆₀ N ₅₄ La ₂₄ Na ₆ Ni ₃₀ O ₃₄₈
fw	11 587.96	10 009.51	10 220.24	13 505.82
<i>T</i> (K)	123(2)	223(2)	223(2)	113(2)
cryst syst	trigonal	hexagonal	cubic	cubic
space group	<i>R</i> ³	<i>P</i> 6(3)/ <i>m</i>	<i>P</i> 2(1)3	<i>P</i> <i>a</i> ³
<i>a</i> , Å	29.927(3)	21.6766(14)	33.9178(8)	33.8871(13)
<i>b</i> , Å	29.927(3)	21.6766(14)	33.9178(8)	33.8871(13)
<i>c</i> , Å	39.912(8)	36.176(5)	33.9178(8)	33.8871(13)
α, deg	90	90	90	90
β, deg	90	90	90	90
γ, deg	120	120	90	90
<i>V</i> , Å ³	30 958(8)	14 721(2)	39 019.6(16)	38 914(3)
<i>Z</i>	3	2	4	4
<i>D</i> _c (g cm ⁻³)	1.865	2.258	1.740	2.305
μ (mm ⁻¹)	3.459	4.674	3.694	4.127
data/params	12 017/652	8048/663	21 693/1280	11 405/797
θ (deg)	1.53–25.00	2.24–25.00	1.20–25.00	1.34–25.00
obsd refls	10148	6210	10939	9185
<i>R</i> 1 [<i>I</i> > 2σ(<i>I</i>)]	0.0498	0.0980	0.0774	0.0522
w <i>R</i> 2 (all data)	0.1375	0.2229	0.2054	0.1509

though communicated recently,¹⁵ are included here to help put the new compounds into context for comparisons of both the molecular structures and magnetic properties of these closely related clusters.

Experimental Section

Chemicals were used as purchased from commercial vendors without further purification. The hydrothermal syntheses were carried out in polytetrafluoroethylene-lined stainless steel containers under autogenous pressure. The C, H, and N microanalyses were carried out with a Vario EL III elemental analyzer. Magnetic measurements were carried out with a Quantum Design SQUID MPMS magnetometer working in the 2–300 K range. The magnetic field was 1000 G. Diamagnetic corrections were made with Pascal's constants.

Synthesis. [La₂₀Ni₃₀(C₄H₅NO₄)₃₀(CO₃)₆(NO₃)₆(OH)₃₀(H₂O)₁₂][CO₃]₆·72H₂O (**1**). An aqueous mixture was prepared by mixing Ni(NO₃)₂·6H₂O (0.436 g, 1.50 mmol), La(NO₃)₃·6H₂O (0.433, 1.00 mmol), and iminodiacetic acid (0.266 g, 2.00 mmol) in 15 mL of deionized water. The pH of this solution was adjusted to ca. 4 by the addition of NaOH (aqueous 1.0 M). This solution was then sealed in a 25-mL Teflon-lined stainless steel container. The container and its contents were heated to 180 °C and maintained at this temperature for 100 h. At a rate of 3 °C h⁻¹, the system was allowed to cool to 100 °C and held there for 16 h, after which cooling continued at the same rate to room temperature. Any insoluble residue was filtered off, and the blue filtrate was allowed to evaporate at room temperature. The product was obtained as cube-shaped dark-blue crystals after 3 months (yield 30.0%). Anal. Calcd for C₁₃₂H₃₄₈La₂₀N₃₆Ni₃₀O₂₈₈ (fw = 11561.56): C, 13.70; H, 3.03; N, 4.36. Found: C, 13.78; H, 2.95; N, 4.16. The Ni/La molar ratio was determined to be 30:19.8 by analysis using an inductively coupled plasma atomic emission spectrometer. This value is consistent with the formula established by crystallographic analysis.

[Pr₂₀Ni₂₁(C₄H₅NO₄)₂₁(OH)₂₄(C₂H₂O₃)₆(C₂O₄)₃(NO₃)₉(H₂O)₁₂](NO₃)₉·42H₂O (**2**). When otherwise identical procedures were adopted and Pr(NO₃)₃ was started with in place of La(NO₃)₃, compound **2** was obtained as block-shaped green crystals in about

10% yield. Anal. Calcd for C₁₀₂H₂₂₅Pr₂₀N₃₉Ni₂₁O₂₃₄ (fw = 9793.33, based on 30 water molecules of crystallization): C, 12.51; H, 2.32; N, 5.58. Found: C, 12.52; H, 2.36; N, 5.52.

[Nd₂₀Ni₂₁(C₄H₅NO₄)₂₁(OH)₂₄(C₂H₂O₃)₆(C₂O₄)₃(NO₃)₉(H₂O)₁₂](NO₃)₉·50H₂O (**3**). When otherwise identical procedures were adopted and Nd(NO₃)₃ was started with in place of La(NO₃)₃, compound **3** was obtained as block-shaped blue crystals in about 15% yield. Anal. Calcd for C₁₀₂H₂₆₅Nd₂₀N₃₉Ni₂₁O₂₅₄ (fw = 10112.15, based on 44 water molecules of crystallization): C, 12.12; H, 2.52; N, 5.40. Found: C, 12.28; H, 2.52; N, 5.05.

{[La₄Ni₅Na(C₄H₅NO₄)₅(CO₃)(NO₃)₄(OH)₅(H₂O)₅][CO₃·10H₂O]}_∞ (**4**). When otherwise identical procedures were adopted and 2.00 mmol instead of 1.00 mmol of La(NO₃)₃ was used, compound **4** was isolated as block-shaped blue crystals in about 20% yield. Anal. Calcd for C₂₂H₆₀La₄N₉NaNi₅O₅₈ (fw = 2246.49): C, 11.75; H, 2.69; N, 5.61. Found: C, 11.74; H, 2.71; N, 5.60.

X-ray Crystallography. Data were collected on a Bruker SMART Apex CCD diffractometer using graphite-monochromatized Mo Kα radiation (λ = 0.710 73 Å) at 123 K for **1**, 223 K for **2** and **3**, and 113 K for **4**. Absorption corrections were applied using the multiscan program *SADABS*. The structures were solved by direct methods (*SHELXTL*, version 5.10),²⁶ and the non-H atoms were refined anisotropically by a full-matrix least-squares method on *F*². The H atoms of an organic ligand were generated geometrically (C–H = 0.96 Å; N–H = 0.90 Å). Crystal data, as well as details of the data collection and refinement, for compounds **1–4** are summarized in Table 1.

Results and Discussion

Synthesis. We sought the preparation of heterometallic complexes containing both transition-metal and lanthanide ions using a one-pot synthesis under hydrothermal conditions. When a mixture of Ni(NO₃)₂·6H₂O, Ln(NO₃)₃·6H₂O (Ln = La, Pr, and Nd), and IDA is utilized, three discrete clusters, [La₂₀Ni₃₀(IDA)₃₀(CO₃)₆(NO₃)₆(OH)₃₀(H₂O)₁₂](CO₃)₆·72H₂O (**1**), [Ln₂₀Ni₂₁(C₄H₅NO₄)₂₁(OH)₂₄(C₂H₂O₃)₆(C₂O₄)₃(NO₃)₉(H₂O)₁₂](NO₃)₉·*n*H₂O [C₂H₂O₃ is the alkoxide form of glycolate; Ln = Pr (**2**), *n* = 42; Nd (**3**), *n* = 50], and one three-dimensional cluster assembly, {[La₄Ni₅Na(IDA)₅(CO₃)-

(26) Bruker. *SHELXTL*, version 5.10; Bruker AXS Inc.: Madison, WI, 1997.

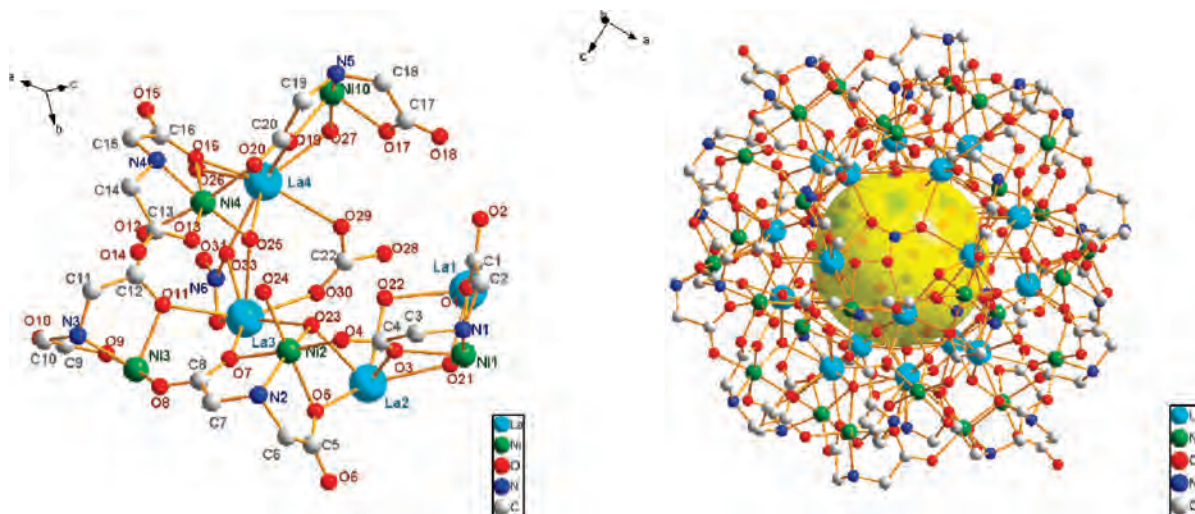


Figure 2. Left: Asymmetric unit of compound **1**, less the counterion CO_3^{2-} and crystallization water. Right: Crystal structure of **1** with H atoms and the counterion CO_3^{2-} removed for clarity.

$(\text{NO}_3)_4(\text{OH})_5(\text{H}_2\text{O})_5[\text{CO}_3] \cdot 10\text{H}_2\text{O}$) $_{\infty}$ (**4**), were obtained. Clusters **1–3** were synthesized using different lanthanide salts under otherwise identical conditions. That clusters of two distinct types were obtained indicates that the cluster structure is sensitively dependent on the identity of the lanthanide ions. The starting Ln/Ni/IDA ratio has also been found to be critical in determining the structure of the final product. Using an extra 1 mol equiv of the lanthanide starting material afforded compound **4**, a cluster assembly constructed by individual clusters interlinked by units of $\text{NaNO}_3/\text{La}(\text{NO}_3)_3$.

Iminodiacetate and its various derivatives are multifunctional,²⁷ not only serving to coordinate Ni^{II} and Ln^{III} ions by chelating and bridging interactions but also acting as a supporting ligand to control the hydrolysis of the lanthanide ions so that finite-sized, hydroxo-bridged polynuclear complexes can be formed. This ligand has been applied for the synthesis of a trigonal-prismatic LnCu_6 cluster by Gao and co-workers.²⁸ More recently, the first three-dimensional interpenetrating 3d–4f coordination polymers have been obtained by a hydrothermal reaction using a starting mixture of IDA, Ln_2O_3 ($\text{Ln} = \text{Sm}$ and Eu), and $\text{Cr}(\text{NO}_3)_3$, during which IDA was partially decomposed to give coordinating oxalate anions.²⁹ It is noteworthy that an increasing number of reports of in situ formation of new ligands due to hydrothermal decomposition of certain organic ligands has appeared in the literature.³⁰ The decomposition products, frequently small molecular anionic species, act as counterions and/or ligands to assist in the assembly of the resulting

complexes. They are critically important for the assembly of the generally unexpected polynuclear structures of the final product(s).

Hydrothermal decomposition of IDA in the present case led to the formation of oxalate in the synthesis of the two isostructural clusters, **2** and **3**. Decomposition products include also glycolate in its alkoxide form (in **2** and **3**) and carbonate (in **1** and **4**). The identity of the glycolate was inferred from the Ln–O bond lengths, and charge balancing necessitates the glycolate to be in its deprotonated (alkoxide) form. To our best knowledge, these are the first observations of such transformations. The overall composition of the clusters is supported by the satisfactory elemental analyses. All of these IDA-derived species are metal-coordinating, with carbonate also serving as counteranions in **1** and **4**.

Structural Description. The crystal structure of **1** consists of a well-separated cationic cluster of $[\text{La}_{20}\text{Ni}_{30}(\text{C}_4\text{H}_5\text{NO}_4)_{30}(\text{CO}_3)_6(\text{NO}_3)_6(\text{OH})_{30}(\text{H}_2\text{O})_{12}]^{6+}$, uncoordinated carbonate ions, and water molecules of crystallization. The asymmetric unit of the structure, less the carbonate counteranions, is shown in Figure 2, left, while the complex structure of **1** is depicted in Figure 2, right.

The Ni^{II} ions form the outer shell structure and are connected exclusively by the carboxylate groups of the IDA ligands in an anti–syn fashion (Figure 3).³¹ Ni1, Ni3, and Ni10 are each connected with four neighboring Ni centers, whereas Ni2 or Ni4 has only three Ni neighbors (For atomic labelings, see Figure S1, Supporting Information.) The local coordination environment of the Ni^{II} ions is best described as a distorted octahedron. Despite some subtle differences, a number of common features are shared. Each Ni^{II} features the contribution of three coordinating atoms from one IDA ligand (an N atom and two O atoms, one from each of its carboxylate groups). These atoms are disposed in a meridional arrangement for the coordination of Ni4, and one of

(27) Schmitt, W.; Murugesu, M.; Goodwin, J. C.; Hill, J. P.; Mandel, A.; Bhalla, R.; Anson, C. E.; Heath, S. L.; Powell, A. K. *Polyhedron* **2001**, *20*, 1687.

(28) (a) Liu, Q.-D.; Li, J.-R.; Gao, S.; Ma, B.-Q.; Kou, H.-Z.; Ouyang, L.; Huang, R.-L.; Zhang, X.-X.; Yu, K.-B. *Eur. J. Inorg. Chem.* **2003**, *4*, 731. (b) Liu, Q.-D.; Gao, S.; Li, J.-R.; Zhou, Q.-Z.; Yu, K.-B.; Ma, B.-Q.; Zhang, S.-W.; Zhang, X.-X.; Jin, T.-Z. *Inorg. Chem.* **2000**, *39*, 2488.

(29) Zhai, B.; Yi, L.; Wang, H.-S.; Zhao, B.; Cheng, P.; Liao, D.-Z.; Yan, S.-P. *Inorg. Chem.* **2006**, *45*, 8471.

(30) (a) Chen, X.-M.; Tong, M.-L. *Acc. Chem. Res.* **2007**, *40*, 162. (b) Zhang, X.-M. *Coord. Chem. Rev.* **2005**, *249*, 1201.

(31) (a) Bandyopadhyay, S.; Das, A.; Mukherjee, G. N.; Cantoni, A.; Bocelli, G.; Chaudhuri, S.; Ribas, J. *Inorg. Chim. Acta* **2004**, *357*, 3563. (b) Wu, Y.; Long, L.-S.; Huang, R.-B.; Zheng, L.-S.; Ng, S. W. *Acta Crystallogr., Sect. E* **2003**, *E59*, m390.

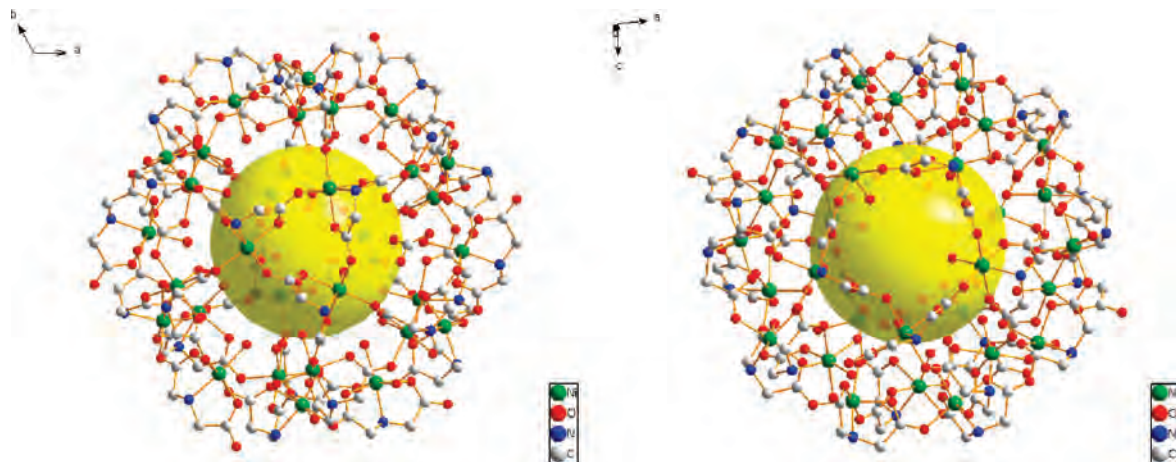


Figure 3. Framework of the 30 Ni^{II} ions interconnected with 30 iminodiacetate (IDA) ligands, viewed from along two different axes. IDA ligands coordinate the Ni^{II} ions exclusively in anti-syn fashion, while a μ_3 -OH group completes the coordination sphere of each Ni^{II} ion. The triangular (left) and pentagonal (right) faces of the Ni₃₀ icosidodecahedron, one for each, are clearly shown in the front.

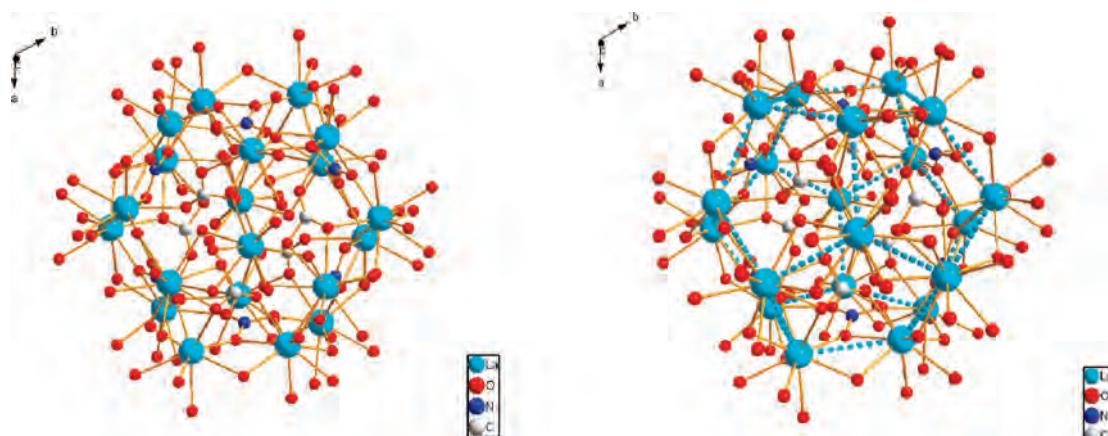


Figure 4. Coordination sphere of La^{III}, featuring coordinating O atoms from the IDA ligands, μ_3 -OH, μ_2 -H₂O, CO₃²⁻, and NO₃⁻ groups (left). The pentagonal faces of the La₂₀ dodecahedron are clearly shown (right).

the carboxylate O atoms of this particular IDA ligand remains uncoordinated. In contrast, the corresponding IDA ligands for the other Ni^{II} ions have their three coordinating atoms positioned in a facial configuration, with the two remaining carboxylate O atoms coordinating neighboring Ni^{II} ions in the aforementioned anti-syn fashion. Other common features include the occupation of the position trans to the IDA N atom by a μ_3 -OH group. The rest of the coordination sphere is fulfilled either by two IDA carboxylate O atoms (for Ni1, Ni3, Ni4, and Ni10) or by one carboxylate O atom and a terminal aqua ligand (for Ni2). The average distances of Ni–N (2.079 Å) and Ni–O (IDA, 2.049 Å) are in good agreement with other crystallographically characterized Ni–IDA systems.³¹ The Ni–O distances (μ_3 -OH, 2.036 Å; terminal aqua ligand, 2.072 Å) are also within the ranges expected for such a coordination.^{28,29}

The La^{III} ions form the inner shell and are coordinated/connected by μ_3 -OH, μ_2 -H₂O, CO₃²⁻, and NO₃⁻ groups (Figure 4; see also Figure S1 in the Supporting Information for atomic labelings). The coordination geometry of individual La^{III} ions is not as well defined because of flexible coordination of the lanthanides. La2 is decacoordinate, while the other La^{III} ions are nonacoordinate. Each of the La atoms features the coordination of three μ_3 -OH groups in addition

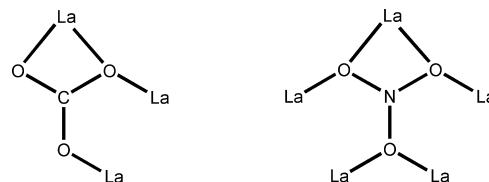


Figure 5. Coordination modes of CO₃²⁻ (left) and NO₃⁻ (right) in 1.

to contributions by two (for La3) or three carboxylate O atoms (for La1, La2, and La4) of IDA ligands. Furthermore, the coordination sphere of all La^{III} ions except La1 contains carbonato and nitrate ligands. The coordination mode of the carbonato ligand (Figure 5, left) has been reported in a number of structures³² but only once with a lanthanide ion.³³ As for the nitrate ligand, there exists only one precedent in the literature, wherein the ligand coordinate Hg^{II} centers in the same fashion as that found in the present case (Figure 5, right)³⁴ but never before with lanthanide ions. The closest example is the one reported recently by Yan and co-workers,

(32) (a) Fu, H.; Chen, W.; Fu, D.; Tong, M.; Chen, X.; Ji, N.; Mao, Z. *Inorg. Chem. Commun.* **2004**, *7*, 1285. (b) Laborda, S.; Clerac, R.; Anson, C. E.; Powell, A. K. *Inorg. Chem.* **2004**, *43*, 5931. (c) Cernak, J.; Ferencova, B.; Zak, Z. *Polyhedron* **2005**, *24*, 579.

(33) Natrajan, L.; Pecaut, J.; Mazzanti, M. *Dalton Trans.* **2006**, 1002.

(34) Zinn, A. A.; Knobler, C. B.; Harwell, D. E.; Hawthorne, M. F. *Inorg. Chem.* **1999**, *38*, 2227.

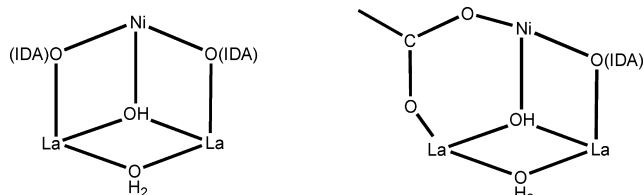


Figure 6. Depiction of the local linkage between the outer framework of Ni^{II} ions and the inner shell of La^{III} ions. Two different types of bridging interaction of the IDA ligand are shown.

where a bridging μ_4 -NO₃⁻ coordinates four La atoms in a [4.221] fashion.³⁵ For La1 and La2, three and one bridging aqua ligands are seen in their respective coordination spheres. The La–O distances of various kinds (μ_3 -OH, bridging H₂O, CO₃²⁻, NO₃⁻, or IDA) are all within the normal range.

The two metal spheres are linked by bridging IDA ligands and triply bridging μ_3 -OH groups. Except for Ni4, each Ni^{II} ion and its two nearest La^{III} neighbors, together with their bridging O atoms, form a core that approximates an incomplete cube whose component two diamond-shaped NiLaO₂ units and one La₂O₂ unit join together at a μ_3 -OH group (Figure 6, left). For Ni4, one of the aforementioned NiLaO₂ units is replaced by a six-membered ring consisting of the two metal ions separated on one side by a μ_3 -OH and by a bridging IDA carboxylate group on the other side (Figure 6, right). The shortest La \cdots La distances range from 4.089 to 4.198 Å (av 4.148 Å), the Ni \cdots Ni distances from 5.144 to 5.450 Å (av 5.256 Å), and the shortest La \cdots Ni separation from 3.531 to 4.183 Å (av 3.669 Å).

The structure of the cationic cluster of **2** is shown in Figure 7. The dual-shell framework structure may be viewed as constructed from two identical bowl-shaped fragments, each featuring a bowl of Pr₁₀ stacked up in the outer bowl of Ni₉. The two Ni₉ bowls are joined together by three Ni^{II} ions (Ni4, Ni4A, and Ni4B) and bridging NO₃⁻ and oxalate ligands (Supporting Information, Figure S2). As such, a closed-shell structure is formed, holding inside the Pr₂₀ unit. The cluster core featuring an outer shell of 21 Ni^{II} ions encapsulating an inner shell of 20 Pr^{III} ions is depicted in Figure 8. Though distinctly different, this core structure can be viewed as being formally transformed from that of **1** (Figure 9). By removal of 9 uniquely positioned Ni^{II} ions from the outer Ni^{II} shell of **1**, followed by a rotation of 60° of the red-colored set of Ni^{II} ions with respect to the green-colored set, the Ni₂₁ framework of **2** is generated (Figure 9). The formal transformation necessary to obtain the inner Pr₂₀ core from the dodecahedron of La^{III} of **1** is even more straightforward; a proper C₆ rotation of the red-colored fragment with respect to the light-blue set is adequate.

The Ni^{II} ions within the outer shell, as in the case of **1**, are connected exclusively via carboxylate groups of the IDA ligands in the anti-syn fashion (Figure 10). Ni1 and Ni2 are each connected with three neighboring Ni centers, whereas Ni2 and Ni4 have two and four Ni neighbors, respectively. (See Figure S2, Supporting Information for atomic labeling.) The whole Ni shell may be viewed as being

constructed by using the three middle Ni^{II} ions (Ni4, Ni4A, and Ni4B), each linking four Ni^{II} neighbors to give a trigonal-prism-shaped arrangement, followed by capping of each of the two triangular faces with an Ni₃ fragment, which itself forms an equilateral triangle with bridging IDA ligands as its side, also in the anti-syn fashion.

The coordination geometry of Ni^{II} is distorted octahedron. Common features shared by all Ni^{II} ions include coordination by one triply bridging OH group and one tridentate IDA ligand; the latter contributes its N and two O atoms, one from each of its carboxylate groups. These three coordinating atoms are arranged facially in the distorted octahedral coordination sphere, with the N atom being trans to the μ_3 -OH group. For Ni3, one of the carboxylate O atoms of this particular IDA ligand remains uncoordinated. That one of the two positions trans to the coordinating O atoms of the tridentate IDA is occupied by a carboxylate O atom from a second IDA ligand constitutes the other common feature in the coordination of Ni^{II} ions. The last coordination site of Ni1, Ni2, and Ni3 is respectively filled by a carboxylate O atom of a third IDA, a carboxylate O atom of glycolato, and a terminal aqua ligand. The local coordination of the bowl-linking Ni4 is identical with that of Ni1. The average Ni–N and Ni–O (IDA, glycolate, μ_3 -OH, and terminal aqua ligand) distances are all within the ranges expected for such a coordination.

The Pr^{III} ions within the inner shell are connected by μ_3 -OH, μ_2 -H₂O, oxalate, and NO₃⁻ groups (Figure 11). The coordination geometry of the Pr^{III} ions is not as systematic as that of Ni^{II}, but they are all nonacoordinate. Six different types of ligands are involved, namely, IDA, μ_3 -OH groups, NO₃⁻, glycolate, oxalate, and water molecules, but only the first three are found in the coordination spheres of all four unique Pr^{III} ions. The μ_3 -OH group bridges one Ni^{II} and two Pr^{III} ions, forming one vertex of a distorted cube. Each of the IDA ligands coordinates one Pr^{III} ion in a monodentate fashion using one of the non-Ni^{II}-coordinating carboxylate O atoms. However, the coordination modes of the nitrate ligand are not all the same. In addition to the mode found in the structure of **1** (Figure 5, right), a more common mode using two of the three O atoms to form a Pr–O–N–O–Pr bridge is also present in the structure. The coordination sphere of Pr1 features two IDA ligands, two μ_3 -OH groups, one glycolate O, and three nitrate ligands contributing four total coordinating O atoms. For Pr2, there are IDA ligands, three μ_3 -OH groups, one bridging aqua ligand, one nitrate, and one oxalate ligand. The coordination of Pr3, because of its crystallographically unique position, is much less complicated when compared with the other Pr^{III} ions. IDA, a μ_3 -OH group, and nitrate, three of each, are found in its coordination sphere. Pr4 is unique in that its coordination sphere contains all different types of ligands. In addition to the two “regular” IDA and one μ_3 -OH ligands, there are one terminal aqua ligand, one chelating glycolate via a five-membered ring involving the alkoxide O atom of the glycolato ligand, one nitrate, and a chelating oxalate. The oxalate group, being almost planar, acts as bis-bidentate and monodentate through two O atoms in cis positions (Figure

(35) Xu, J.-Y.; Zhao, B.; Bian, H.-D.; Gu, W.; Yan, S.-P.; Cheng, P.; Liao, D.-Z.; Shen, P.-W. *Cryst. Growth Des.* **2007**, *7*, 1044.

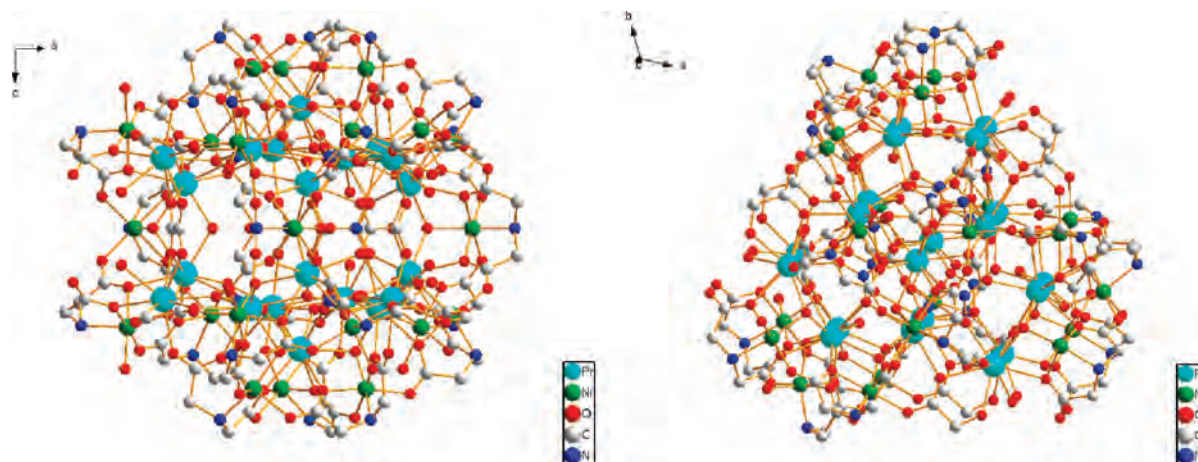


Figure 7. Crystal structure of the cationic cluster of compound **2**, viewed along two different directions.

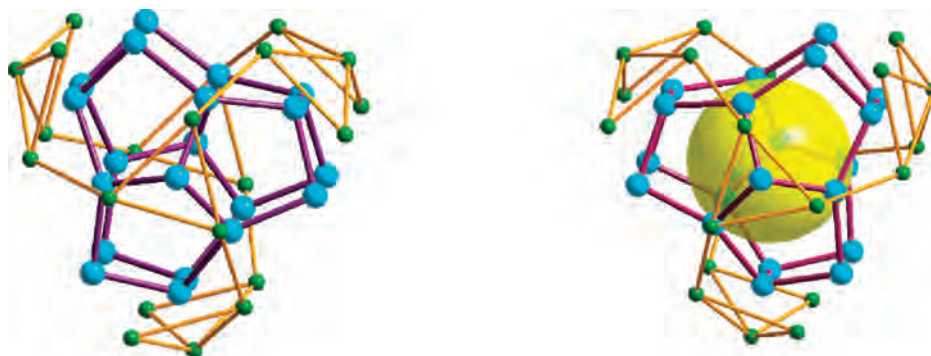


Figure 8. Cluster core structure of **2** showing an outer Ni₂₁ framework encapsulating an inner Pr₂₀ framework. Color legends: Ni, green; Pr, cyan.

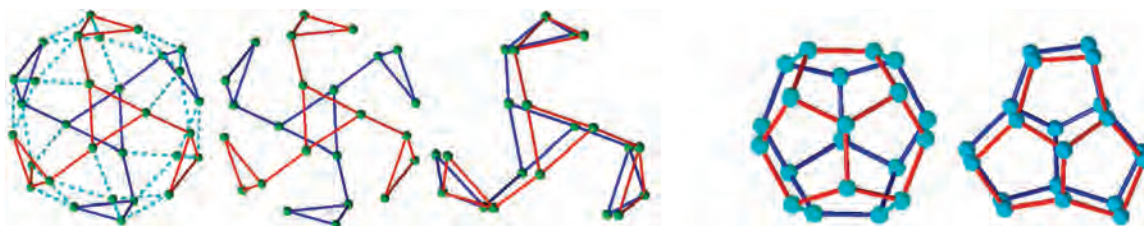


Figure 9. Depiction of the formal transformations toward the making of the inner and outer frameworks of **2** from respective polyhedra of cluster **1**. Color legends: Ni, green; Ln, cyan.

12, left). Such a coordination mode, though not uncommon,³⁶ has only been shown in one lanthanide complex.³⁷ The C–C and C–O bonds within these ligands are as expected. The Pr–O distances of various kinds (μ_3 -OH, μ_2 -H₂O, NO₃[−], oxalate, glycolate, or IDA) are all within the normal range expected for such bonds.

The two metal spheres are linked by bridging IDA ligands and triply bridging μ_3 -OH groups. Like in the case of **1**, each Ni^{II} ion and its two nearest Pr^{III} neighbors, together with their bridging O atoms, form a core that approximates an incomplete cube composed of two units of diamond-shaped NiPrO₂ and one unit of Pr₂O₂ joined at a shared triply bridging OH group. Bridging the two distinct shells are the glycolato ligands: One Ni^{II} and two Pr^{III} ions are connected in a previously unknown fashion (Figure 12, right). It is because of such extensive bridging interactions that the

sophisticated, dual-shell framework structure is generated. The shortest Pr–Pr distances range from 3.969 to 4.223 Å (av 4.087 Å), the Ni–Ni distances from 5.195 to 5.276 Å (av 5.217 Å), and the shortest Pr–Ni separation from 3.478 to 3.655 Å (av 3.569 Å).

Compound **3** is structurally very similar to **2**, with the differences being in the metric values of the bond lengths and angles anticipated for different lanthanide ions used and in the number of water molecules of crystallization (Supporting Information, Figure S3). The shortest Nd···Nd distances range from 3.969 to 4.200 Å (av 4.079 Å), the Ni···Ni distances from 5.197 to 5.265 Å (av 5.208 Å), and the shortest Nd···Ni separation from 3.478 to 3.641 Å (av 3.556 Å).

The overall structure of **4** is a rather complex three-dimensional assembly built by discrete cationic clusters. These clusters have 3-fold inversion rotational symmetry. The cluster framework is identical with that of **1** except that there is an additional La atom (La₆) within the La₂₀ cage

(36) Armentano, D.; De Munno, G.; Lloret, F.; Julve, M. *CrystEngComm* **2005**, *7*, 57.

(37) Thomas, P.; Trombe, J. C. *J. Chem. Crystallogr.* **2000**, *30*, 633.

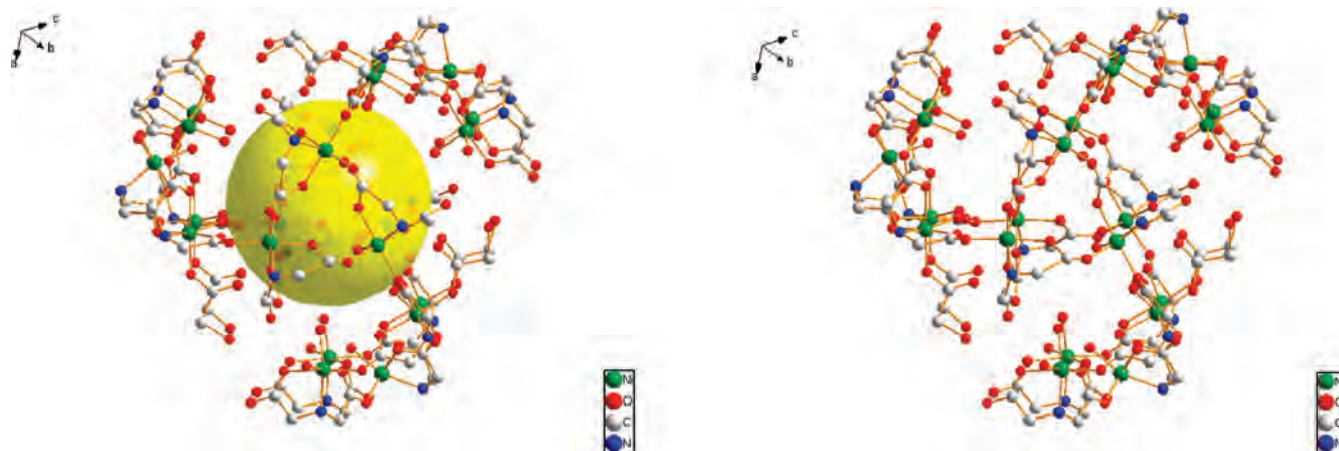


Figure 10. Framework of the 21 Ni^{II} ions interconnected with 21 iminodiacetate (IDA) ligands. IDA ligands coordinate the Ni^{II} ions exclusively in an anti-syn fashion, while a μ_3 -OH group completes the coordination sphere of each Ni^{II}. The 3-fold rotational symmetry can be clearly seen from the structure.

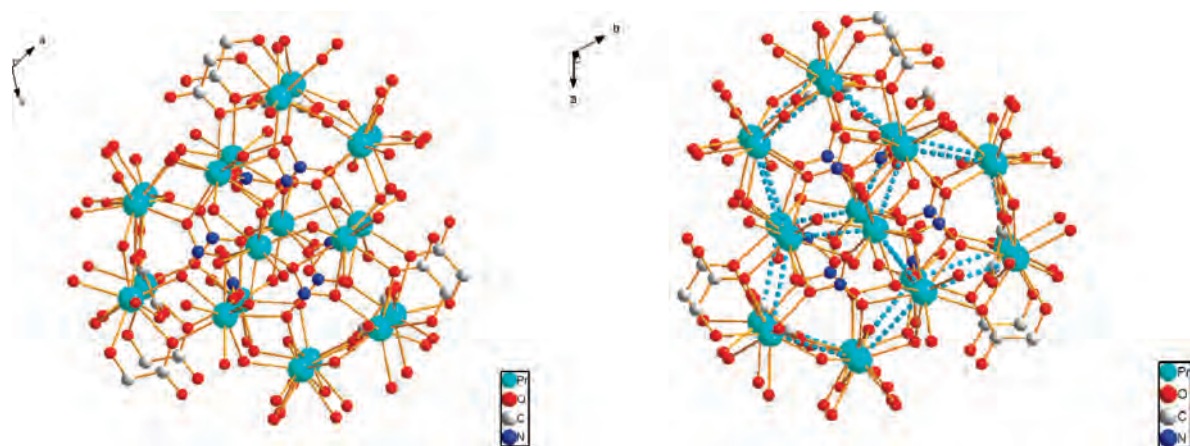


Figure 11. Coordination sphere of Pr^{III}, featuring coordinating O atoms from the IDA ligands, μ_3 -OH, μ_2 -H₂O, oxalate, and NO₃⁻ groups (left). The polyhedral framework structure of the Pr₂₀ core is clearly shown (right).

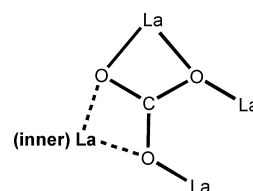
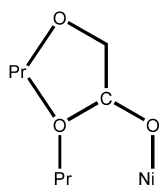
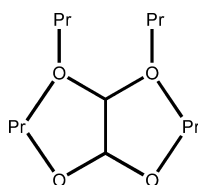


Figure 12. Coordination modes of oxalato (left) and deprotonated glycolato (right) ligands in **2**.

Figure 13. Coordination mode of the carbonato ligands in **2**. The portion of the coordination indicated by the solid lines is the same as that observed in compound **1** (Figure 5).

(Supporting Information, Figure S4). This unique La^{III} ion is attached from within to the La₂₀ dodecahedron via bridging interactions mediated by three chelating carbonate groups. The coordination mode of these carbonate ligands, shown in Figure 13, is quite common in lanthanide complexes.³⁸ We note that the present μ_4 -carbonato coordination can be generated formally by an additional chelation, indicated by dashed lines in Figure 13, of the carbonate ligands shown in Figure 5. The coordination sphere of La₆ is then completed by six aqua ligands that are located opposite to these carbonate ligands. As such, the coordination number is 12. Crystallographically the best results were obtained by refining La₆ as being disordered across the inversion center with 60%

occupancy on one side and 40% on the other. The shortest La \cdots La distances range from 4.089 to 4.200 Å (av 4.146 Å), the Ni \cdots Ni distances from 5.125 to 5.470 Å (av 5.236 Å), and the shortest La \cdots Ni separation from 3.519 to 4.180 Å (av 3.672 Å).

Each cluster unit branches out by the way of six NaNO₃ units. The binding of the Na⁺ ion by the cluster is achieved by using the free carboxylate O atom of the unique IDA ligand, detailed above in the structural description of **1**. Each NaNO₃ unit is further “stationed” onto a different locally central La(NO₃)₃ unit (Figure 14). Each La(NO₃)₃ unit is engaged in this kind of connection by having three surrounding NaNO₃ units. As such, a complex three-dimensional network structure featuring the individual cluster linked by La(NO₃)₃/NaNO₃ units is formed. The apparent “gaps” left

(38) (a) Serre, C.; Marrot, J.; Férey, G. *Inorg. Chem.* **2005**, *44*, 654. (b) Trombe, J. C.; Roméro, S.; Mosset, A. *Polyhedron* **1998**, *17*, 2529. (c) Müller-Buschbaum, K. *Z. Anorg. Allg. Chem.* **2002**, *628*, 1761.

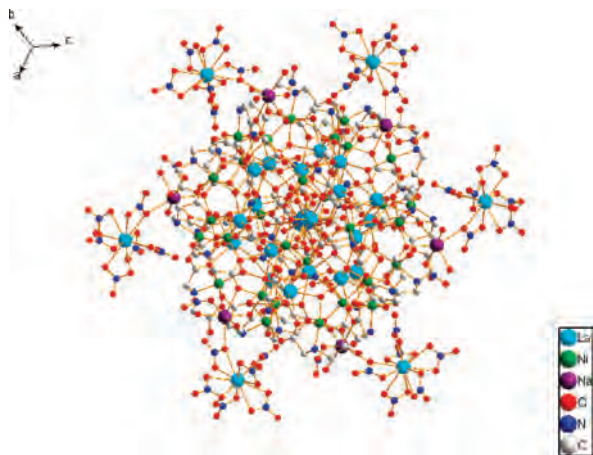


Figure 14. Partial showing of the crystal structure of the cluster network **4**. One discrete cluster, structurally similar to that of **1**, is shown with six network-building $\text{NaNO}_3/\text{La}(\text{NO}_3)_3$ units.

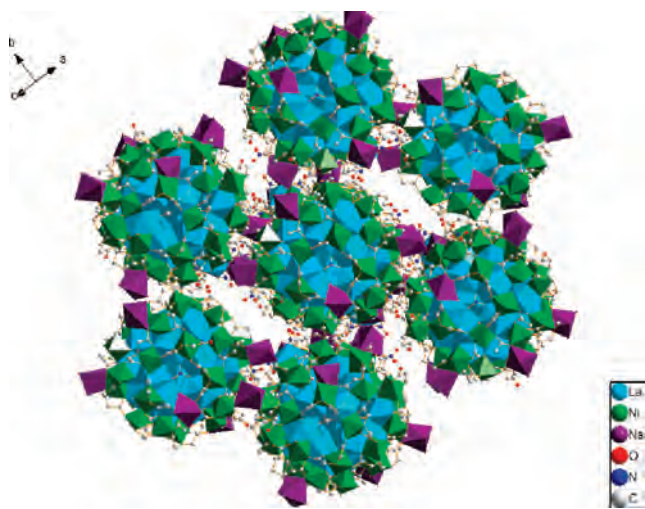


Figure 15. View of the crystal structure of **4**. The coordination spheres of different metal ions are depicted using colored polyhedra.

between the linked clusters are occupied by the *SQUEEZED*³⁹ solvent–water of crystallization (Figure 15).

Magnetic Studies. Magnetic susceptibilities of **1**, measured in an applied field of 1000 Oe over the temperature range of 2–300 K, are shown in Figure 16, left, in the form of $\chi_{\text{M}}T$ versus T . The $\chi_{\text{M}}T$ value of $36.34 \text{ cm}^3 \text{ K mol}^{-1}$ at 300 K corresponds to 30 uncorrelated Ni^{II} ions with μ_{eff} (per Ni) = $3.14 \mu_{\text{B}}$ and $g = 2.22$ (calculated value $36.96 \text{ cm}^3 \text{ K mol}^{-1}$). The susceptibility arises solely from Ni^{II} ($S = 1$) ions that are expected to exhibit spin-only moments modified by the effects of second-order spin–orbit coupling.⁴⁰ Over the temperature range of 34–300 K, $\chi_{\text{M}}T$ remains essentially constant. Upon further lowering of the temperature, $\chi_{\text{M}}T$ increases rapidly and reaches a maximum value of $264.81 \text{ cm}^3 \text{ K mol}^{-1}$ at 16 K. On the basis of this value, the ground-state spin is estimated to be $S = 20$. Upon further lowering of the temperature, a sharp drop is seen, and a value of $73.49 \text{ cm}^3 \text{ K mol}^{-1}$ is reached at 2 K, possibly because of intercluster antiferromagnetic interactions and zero-field

splitting of the ground state. The temperature dependence of the molar susceptibility in the range of 300–100 K is well described by a Curie–Weiss term, $\chi = C/(T - \Theta)$ with $C = 35.46 \text{ cm}^3 \text{ K mol}^{-1}$ and $\Theta = 10.33 \text{ K}$, consistent with ferromagnetic coupling between the Ni^{II} ions.

The field dependence of the magnetization measured at 2.0 K (Figure 16, right), in the form of a M versus H plot, where M and H are magnetization and applied magnetic field, respectively, confirms the high-spin ground state. We note that the Ni^{II} ions, by occupying the vertices of a perfect icosidodecahedron, constitute a highly frustrated spin lattice, analogous to the famous magnetic cluster $\{\text{Mo}_{72}\text{Fe}_{30}\}$.¹⁷ We thus expect our clusters to be intriguing subjects for theoretical studies of magnetism originating from the geometric frustration of spins.⁴¹

Crystallographic analysis clearly shows that the Ni^{II} ions are linked exclusively by carboxylato groups in the syn–anti fashion, for which both weak ferromagnetic⁴² and antiferromagnetic⁴³ interactions have been reported. However, the magnetostructural relationship of such carboxylate-bridged polynickel complexes/clusters has not yet been established. In comparison, on the basis of both experimental and computational work, more agreeable conclusions have been reached regarding how the carboxylate coordination modes dictate the exchange coupling in carboxylate-bridged di- and polynuclear copper(II) complexes.⁴⁴

For complex **2**, the $\chi_{\text{M}}T$ value of $56.11 \text{ cm}^3 \text{ K mol}^{-1}$ at 300 K is close to the value of $57.88 \text{ cm}^3 \text{ K mol}^{-1}$ calculated on the basis of a free-ion approximation for 21 Ni^{II} ($25.88 \text{ cm}^3 \text{ K mol}^{-1}$) and 20 Pr^{III} ($32.00 \text{ cm}^3 \text{ K mol}^{-1}$) in 3H_4 ground state ($J = 4 \text{ Hz}$, $g = 4/5$) ions,⁸ indicating that no strong magnetic exchange interactions exist between these metal ions (Figure 17, left). Upon lowering of the temperature, $\chi_{\text{M}}T$ decreases gradually and reaches a value of $51.12 \text{ cm}^3 \text{ K mol}^{-1}$ at 16 K, after which $\chi_{\text{M}}T$ decreases abruptly and reaches a value of $25.52 \text{ cm}^3 \text{ K mol}^{-1}$ at 2 K. The data over

- (41) (a) Todea, A. M.; Merca, A.; Bögge, H.; van Slageren, J.; Dressel, M.; Engelhardt, L.; Luban, M.; Glaser, T.; Henry, M.; Müller, A. *Angew. Chem., Int. Ed.* **2007**, *46*, 6106. (b) Schröder, C.; Nojiri, H.; Schnack, J.; Hage, P.; Luban, M.; Kögerler, P. *Phys. Rev. Lett.* **2005**, *94*, 017205/1. (c) Müller, A.; Luban, M.; Schröder, C.; Modler, R.; Kögerler, P.; Axenovich, M.; Schnack, J.; Canfield, P.; Bud'ko, S.; Harrison, N. *ChemPhysChem* **2001**, *2*, 517.
- (42) (a) Zhang, J.-J.; Xiang, S.-Ch.; Hu, S.-M.; Xia, S.-Q.; Fu, R.-B.; Wu, X.-T.; Li, Y.-M.; Zhang, H.-S. *Polyhedron* **2004**, *23*, 2265. (b) Wang, S.; Bai, J.; Xing, H.; Li, Y.; Song, Y.; Pan, Y.; Scheer, M.; You, X. *Cryst. Growth Des.* **2007**, *7*, 747. (c) Du, M.; Bu, X.; Guo, Y.; Zhang, L.; Liao, D.; Ribas, J. *Chem. Commun.* **2002**, 1478.
- (43) (a) Lin, X.; Doble, D. M. J.; Blake, A. J.; Harrison, A.; Wilson, C.; Schröder, M. *J. Am. Chem. Soc.* **2003**, *125*, 9476. (b) Murrie, M.; Stoeckli-Evans, H.; Gudel, H. U. *Angew. Chem., Int. Ed.* **2001**, *40*, 1957. (c) Dearden, A. L.; Parsons, S.; Winpenny, R. E. P. *Angew. Chem., Int. Ed.* **2001**, *40*, 151. (d) Benelli, C.; Blake, A. J.; Brechin, E. K.; Coles, S. J.; Graham, A.; Harris, S. G.; Meier, S.; Parkin, A.; Parsons, S.; Seddon, A. M.; Winpenny, R. E. P. *Chem.–Eur. J.* **2000**, *6*, 883. (e) Zheng, L. M.; Whitfield, T.; Wang, X. Q.; Jacobson, A. J. *Angew. Chem., Int. Ed.* **2000**, *39*, 4528. (f) Yukawa, Y.; Aromi, G.; Igarashi, S.; Ribas, J.; Zvyagin, S. A.; Krzystek, J. *Angew. Chem., Int. Ed.* **2005**, *44*, 1997.
- (44) (a) Rodríguez-Fortea, A.; Alemany, P.; Alvarez, S.; Ruiz, E. *Chem.–Eur. J.* **2001**, *7*, 627. (b) Ruiz-Pérez, C.; Hernández-Molina, M.; Lorenzo-Luis, P.; Lloret, F.; Cano, J.; Julve, M. *Inorg. Chem.* **2000**, *39*, 3845. (c) Dey, S. K.; Bag, B.; Mali, K. M. A.; El Fallah, M. S.; Ribas, J.; Mitra, S. *Inorg. Chem.* **2003**, *42*, 4029. (d) Murugesu, M.; Clérac, R.; Pilawa, B.; Mandel, A.; Anson, C. E.; Powell, A. K. *Inorg. Chim. Acta* **2002**, *337*, 328.

(39) Spek, A. L. *Acta Crystallogr.* **1990**, *A46*, C34.

(40) Figgis, B. N. *Introduction to Ligand Fields*; Interscience: New York, 1966.

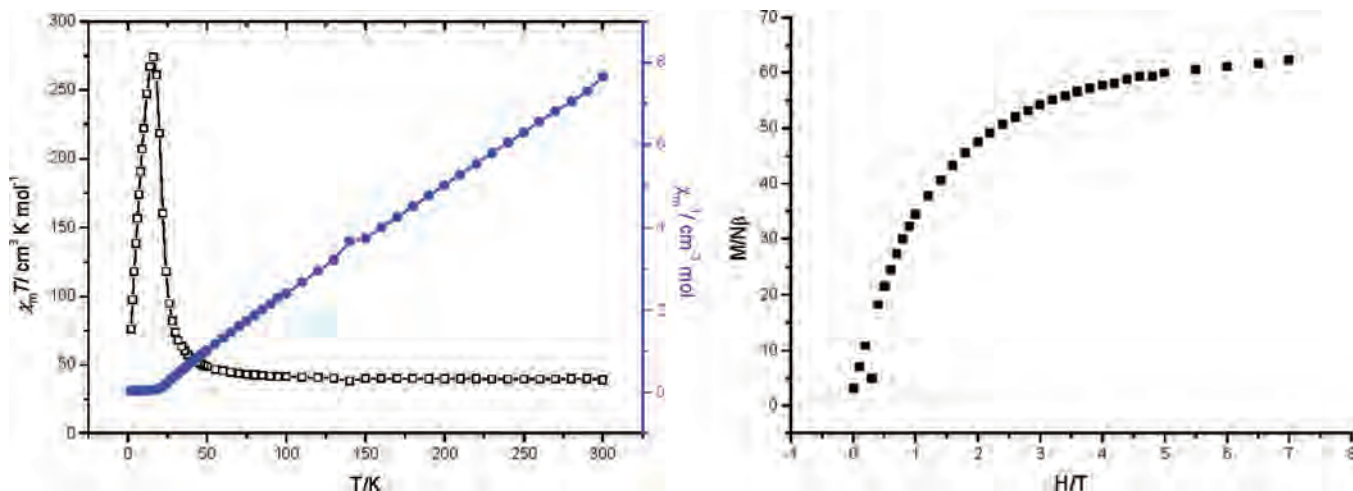


Figure 16. Plots of the temperature dependence of $\chi_M T$ (○) and χ_M^{-1} (●) for complex **1** at 2.0 K and at indicated fields.

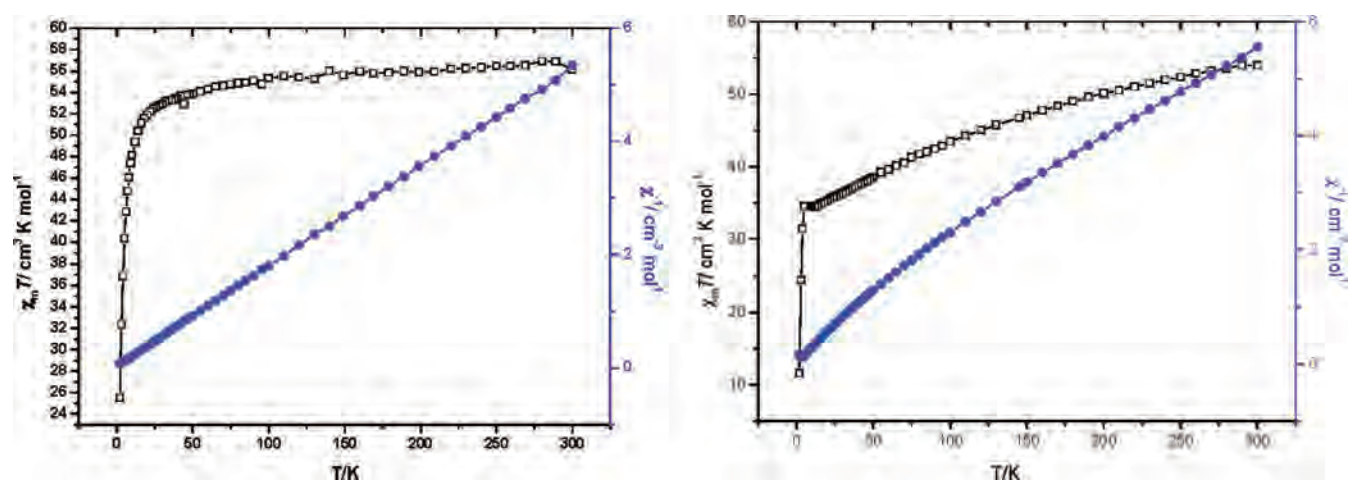


Figure 17. Plots of the temperature dependence of $\chi_M T$ (○) and χ_M^{-1} (●) for complexes **2** (left) and **3** (right).

the whole temperature range of 2–300 K are fitted nicely to the Curie–Weiss equation with $C = 57.1 \text{ cm}^3 \text{ K mol}^{-1}$ and $\Theta = -3.37 \text{ K}$. The negative value of the Weiss constant suggests the presence of antiferromagnetic interactions between neighboring metal centers, probably via superexchange through the bridging ligands. However, it is difficult, if at all possible, to quantify the different contributions of the transition-metal and lanthanide ions because of the highly sophisticated framework structure. In addition, a number of other factors should also be taken into consideration. For example, Pr^{3+} possesses a rather large unquenched orbital angular momentum associated with the internal nature of the valence f orbitals and has orbitally degenerate ground states, which are easily split by spin–orbit coupling and crystal-field effects. Therefore, the decrease in $\chi_M T$ may originate, at least partially, from the thermal depopulation of the highest Stark components derived from the splitting of its free-ion ground state 3H_4 . Furthermore, zero splitting of Ni^{II} may also contribute to the decrease of the $\chi_M T$ product upon lowering of the temperature.⁴⁵

For complex **3**, the $\chi_M T$ value of $53.96 \text{ cm}^3 \text{ K mol}^{-1}$ at 300 K is slightly smaller than the value of $58.68 \text{ cm}^3 \text{ K mol}^{-1}$ calculated on the basis of a free-ion approximation for 21 Ni^{II} ($25.88 \text{ cm}^3 \text{ K mol}^{-1}$) and 20 Nd^{III} ($32.80 \text{ cm}^3 \text{ K mol}^{-1}$) in a $^4I_{9/2}$ ground state ($J = 9/2 \text{ Hz}$, $g = 8/11$) ions (Figure 17, right). Upon lowering of the temperature, $\chi_M T$ decreases sizably and reaches a plateau between 12 and 5 K, with a value of $34.50 \text{ cm}^3 \text{ K mol}^{-1}$. Further lowering of the temperature causes an abrupt decrease of $\chi_M T$, eventually reaching a value of $11.61 \text{ cm}^3 \text{ K mol}^{-1}$ at 2 K. The data over the temperature range of 100–300 K are fitted to the Curie–Weiss equation with $C = 62.7 \text{ cm}^3 \text{ K mol}^{-1}$ and $\Theta = -49.1 \text{ K}$. The magnetic interactions in this complex are qualitatively similar to those of **2**. The decrease of the $\chi_M T$ product upon lowering of the temperature may be rationalized in terms of the ligand-mediated antiferromagnetic couplings between the metal centers, thermal depopulation of the highest Stark components derived from the splitting of the free Nd^{III} ground state by the crystal field, and zero-field splitting of the Ni^{II} ion.

For the three-dimensional cluster network, the χ_M versus T and $\chi_M T$ versus T plots under an applied field of 1000 Oe are shown in Figure 18. The $\chi_M T$ value of $35.75 \text{ cm}^3 \text{ K mol}^{-1}$

(45) (a) Herchel, R.; Boča, R.; Krzystek, J.; Ozarowski, A.; Durán, M.; van Slageren, J. *J. Am. Chem. Soc.* **2007**, *129*, 10306. (b) Konar, S.; Zangrando, E.; Drew, M. G. B.; Ribas, J.; Chaudhuri, N. R. *Dalton Trans.* **2004**, 260.

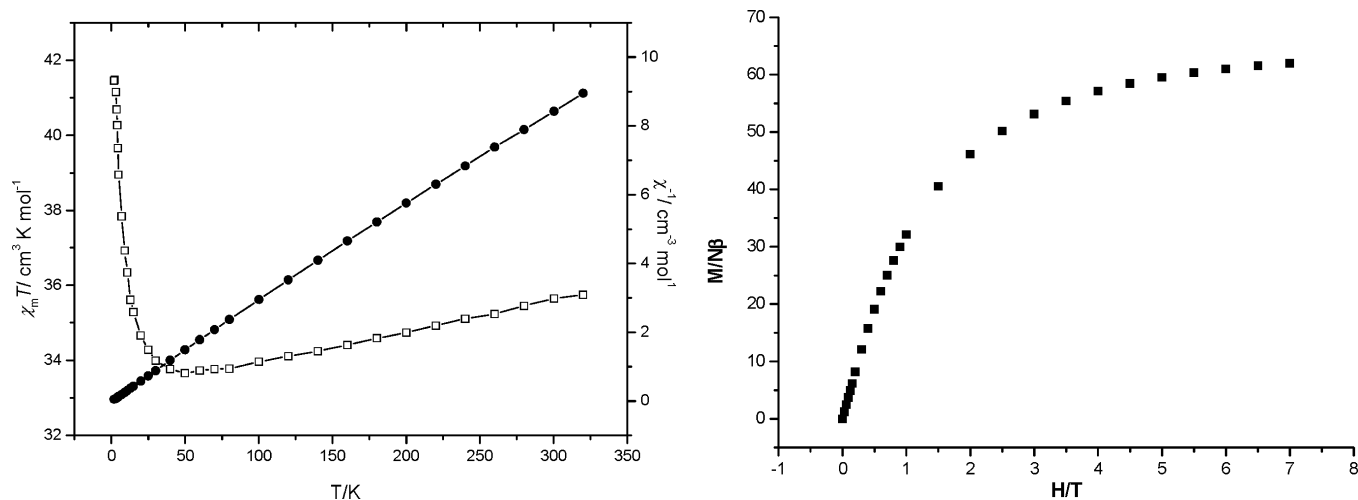


Figure 18. Plots of the temperature dependence of $\chi_M T$ (□) and χ_M^{-1} (●) (left) and magnetization versus H/T for complex **4** at 2.0 K and at indicated fields.

at room temperature is consistent with that expected for 30 magnetically isolated Ni^{II} ions with μ_{eff} (per Ni) = $3.14 \mu_B$ and $g = 2.22$ (calculated $36.96 \text{ cm}^3 \text{ K mol}^{-1}$). The $\chi_M T$ value gradually decreases with lowering of the temperature down to the minimum value of $33.65 \text{ cm}^3 \text{ K mol}^{-1}$ at 50 K and then increases up to the maximum value of $41.45 \text{ cm}^3 \text{ K mol}^{-1}$ at 2 K. Fitting $1/\chi_M$ versus T to the Curie–Weiss law gives a Curie constant $C = 35.7 \text{ cm}^3 \text{ K mol}^{-1}$ and a Weiss temperature $\Theta = -3.6 \text{ K}$. The first decrease of $\chi_M T$ and the negative Θ value suggest the operation of antiferromagnetic interactions between the ions, in contrast to the ferromagnetic interaction observed in the discrete cluster **1**. The origin of this antiferromagnetic behavior is not yet clear. Nevertheless, such effects should be small, and the overall magnetic exchange interaction is still ferromagnetic, leading to the ferrimagnetic behavior of this three-dimensional cluster network.

Summary and Conclusions

We have in this work prepared four cluster-type heterometallic polynuclear complexes featuring both Ni^{II} ions and the lanthanide ions, including La^{III} , Pr^{III} , and Nd^{III} by hydrothermal synthesis, starting from a mixture of the metal salts and an organic ligand iminodiacetic acid. Dual shell-like framework structures featuring an outer shell of Ni^{II} ions encapsulating a smaller and inner shell of Ln^{III} ions have

been obtained for three discrete cluster complexes. It has been found that in situ formation of new ligands due to the decomposition of the organic ligand is common. The newly generated ligands, of both inorganic and organic types, serve to facilitate the formation of the final clusters and to stabilize their structures. The fourth compound is a polymeric three-dimensional cluster assembly formed by bridging interactions between the individual cluster units and branching units of $\text{La}(\text{NO}_3)_3/\text{NaNO}_3$. Magnetic studies have been carried out, and interesting magnetic properties displayed by these structurally related cluster complexes range from ferromagnetic interaction in the cluster containing magnetically silent La^{III} ions (**1**) to the overall ferrimagnetic interactions in the assembly of this cluster type and to antiferromagnetic interactions for the two smaller clusters (**2** and **3**) containing magnetically significant Pr^{III} and Nd^{III} ions.

Acknowledgment. This work was supported by NNSFC (Grant Nos. 20471050, 20531050, and 20423002), the 973 project (Grant No. 2007CB815304) for MSTC. Z.Z. acknowledges support by Xiamen University (Project 985) and by the U.S. NSF (CAREER CHE-0238790).

Supporting Information Available: Figures S1–S5 and CIF files of compounds **1–4**. This material is available free of charge via the Internet at <http://pubs.acs.org>.

IC702079E